Charged particle decay from giant monopole resonance in ^{28}Si

Y. Toba, Y.-W. Lui, and D. H. Youngblood
Cyclotron Institute, Texas A&M University, College Station, Texas 77843

U. Garg
Physics Department, University of Notre Dame, Notre Dame, Indiana 46556

P. Grabmayr,* K. T. Knöpfle, H. Riedesel,† and G. J. Wagner*
Max-Planck-Institut für Kernphysik, 6900 Heidelberg, Federal Republic of Germany
(Received 11 December 1989)

Proton and alpha decay from the giant resonance region of ^{28}Si excited with a 129 MeV alpha particle beam has been measured in coincidence with inelastic alpha particles detected at 0°. The angular correlation data show the presence of decay from both $E0$ and $E2$ giant resonances. The $E0$ giant resonance decays primarily through the α_0, α_1, p_0, and $p_{1,2}$ channels with the branching ratios 18±6 %, 24±8 %, 23±9 %, and 18±8 %, respectively. Substantial direct decay is observed.

INTRODUCTION

After first evidence for the isoscalar giant monopole resonance (GMR) was obtained,[1] extensive studies were performed to identify the GMR in many nuclei over the periodic table and to extract the incompressibility of nuclear matter.[2–4] Most of these studies were done with inelastic scattering of ^{3}He ions and alpha particles with energies between 100 and 170 MeV. To identify the monopole, the experiments were performed at small angles, including 0° where the monopole is excited most strongly. In medium and heavy nuclei (mass number $A > 64$), the GMR has been unambiguously identified at excitation energies $E_x = (70-80)A^{-1/3}$ MeV with width $= 2.5-4$ MeV and contains a large fraction of the energy-weighted sum rule (EWSR) strength.

For $A < 58$, the GMR has been elusive with only a few percent of the sum rule located in most nuclei. Lui *et al.*[5] reported the identification of 66% of the $E0$ EWSR with a width of 4.8 MeV centered at 17.9 MeV in ^{28}Si. ^{28}Si was also investigated by Kailas *et al.*,[6] using 115 MeV proton inelastic scattering, who reported 34% EWSR $E0$ strength in the $E_x = 15.7-24.1$ MeV region, but with a large ambiguity due to the uncertainty in the strength of excitation of the isovector giant dipole resonance (GDR). Kihm *et al.*[7] explored the giant resonance region of ^{28}Si in an (e,e') decay study and report that 20% of the $(e,e'\ \alpha_0)$ cross section arises from $E0$ excitation. Lu *et al.*[8] reported ~90% of the $E0$ EWSR between 11 and 20 MeV in ^{24}Mg. Lebrun *et al.*[9] investigated the nuclei ^{60,58}Ni, ^{56}Fe, ^{27}Al, and ^{12}C with inelastic scattering of 108.5 MeV ^{3}He and found monopole strength of less than 10% EWSR in each nucleus. Duhmal *et al.*[10] report location of 23% of the $E0$ EWSR in ^{58}Ni. In ^{40}Ca, a 0^+ state at $E_x = 14$ MeV containing 6% of the EWSR (Refs. 11 and 12) was identified. Brandenburg *et al.*[13] have performed singles and coincidence measurements on ^{40}Ca using 120 MeV alpha particles and report 30% of the $E0$ EWSR strength fragmented in the broad excitation energy region 10.5–20 MeV.

The GMR lies in a continuum region and can decay by the emission of neutrons, protons, and alpha particles. Measurements of such decay particles in coincidence with inelastically scattered particles exciting the GMR should permit a more confident assignment of the multipolarity through angular correlations, and might provide information on the microscopic structure of the GMR. From the location of particle thresholds and experience with the decay of the giant quadrupole resonance,[14] one would expect the GMR in heavier nuclei to decay primarily by neutron emission; thus we have chosen to investigate charged particle decay of the GMR in ^{28}Si. Further, since the decay of the giant quadrupole resonance (GQR) in ^{28}Si revealed interesting features of intermediate structure and predominance of the direct decay process,[15] it is interesting to investigate whether the decay of the GMR shows a similar direct nature and provides information on the microscopic structure of GMR.

In this paper, we report measurements of charged particles decaying from the giant resonance region of ^{28}Si in coincidence with alpha particles inelastically scattered at 0°. The 0° measurement gives a maximum monopole cross section and an axial symmetry of the angular correlation which makes measurements in one plane sufficient for full determination of the correlation function. This removes one uncertainty in obtaining decay branches from such correlations and, correspondingly, enables a proper definition with fewer measurements.

EXPERIMENTAL PROCEDURE

A 129-MeV alpha particle beam from the Texas A&M University 88 Inch Cyclotron was used to bombard a Si target located in the scattering chamber of the Enge split-pole magnetic spectrograph. The experimental

configuration is illustrated in Fig. 1. The beam was focused on the target in a spot 1 mm high by 2 mm wide, brought into the spectrograph, and stopped by a Faraday cup located 1 m behind the focal plane. The target was a self-supporting natural Si foil with a thickness of 2.05 mg cm^{-2}. Inelastically scattered alpha particles were measured at 0° with a 40-cm long resistive wire proportional counter in the focal plane. The proportional counter was backed by an NE102 scintillator to provide total energy and time of flight signals. Energy-loss signals from both ends of the proportional counter were routed after amplification through two analog to digital converters (ADC's) to a PDP-15 computer, and software division was done to obtain position information.

A 2.0 cm×2.0 cm collimator was used to define the solid angle of the spectrograph. The opening angle was 4.2°, corresponding to a solid angle of 5.3 msr. Considerable care was taken to minimize background contributions from spurious beam particles and from slit scattering. The experimental technique used for the inelastic measurements at 0°, including the electronics setup and precautions against slit scattering, etc., have been described previously.[16]

The decay products were detected by eight silicon detector telescopes located in the scattering chamber. Each telescope consisted of a 70 (or 75) μm ($E1$), a 500 μm ($E2$), and a 2000 μm ($E3$) silicon surface barrier detector. A collimator of 10.7 mm diameter, corresponding to an opening angle of 6.1° and defining a solid angle of 9.0 msr, was used for each detector telescope. The techniques used for particle identification and computer encoding were similar to those described in Ref. 15 and will be described only briefly here.

Linear signals from the three detectors in a telescope were summed together after preamplification; the total energy signal for each telescope was then amplified and routed to the computer through one ADC. In addition to the total energy, a logic signal corresponding to $E1$, $E1*E2$, or $E1*E2*E3$, where Ei means that the ith detector fired, was supplied to the computer for each coincident event in addition to a tag identifying the telescope in which the event occurred.

In the giant resonance region ($E_x = 15-25$ MeV) of ^{28}Si, alpha and proton energies up to 14 MeV are of interest for the decays to the low-lying states of the residual nuclei. The maximum energies of alpha particles which stop in the detectors $E1$, $E2$, and $E3$ are 9.54 MeV, 34.9 MeV, and 82.9 MeV, respectively. For protons they are 2.52 MeV, 8.77 MeV, and 20.5 MeV, respectively.

For on-line spectral monitoring and during off-line data analysis, events of logic $E1$ or $E1*E2$ with a particle energy larger than 9 MeV were sorted as an alpha event and all others were sorted as a proton event. For particle energies below 2.52 MeV, alpha particles and protons were not separated. A time-to-amplitude (TAC) signal, generated by a start signal from the decay detectors and a stop signal from the scintillator, was also routed to the computer through an ADC to classify the event as a true or accidental coincidence. A fast coincidence between signals from the scintillator and any decay detector supplied a gate to the computer. Single data were taken simultaneously by supplying computer gates for a

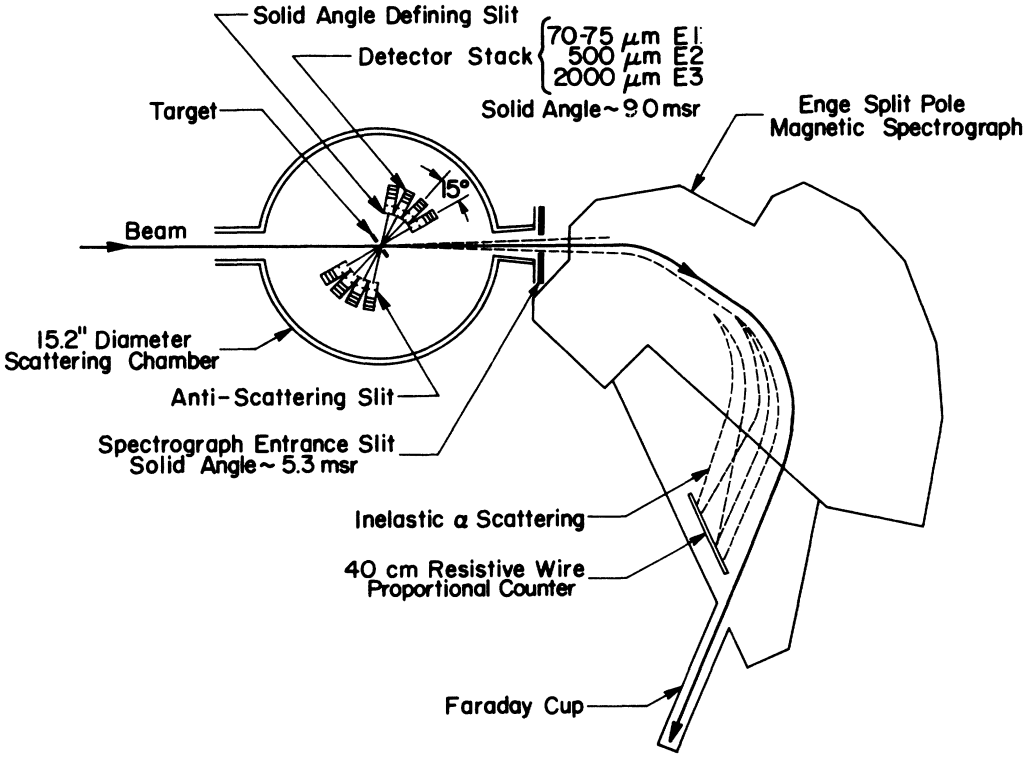

FIG. 1. Experimental configuration for giant resonance decay experiment.

TABLE I. Angles at which the decay detector were located at each run.

Run number	Decay angles (deg)							
1	25.5	40.5	55.5	70.5	109.5	124.5	139.5	154.5
2	48.0	63.0	78.0	93.0	87.0	102.0	117.0	132.0
3	33.0	48.0	63.0	78.0	102.0	117.0	132.0	147.0

fraction (typically 1 in 200) of the singles events. A pulser signal was fed through the single manipulation circuits to the computer during data acquisition and used for a dead-time correction for the entire system. The ADC values, and logic and tag information were stored in event mode on tape for further analysis. In addition, a number of singles and 2D spectra were accumulated live to monitor the experiment. The experiment was performed with beam currents of a 5–8 nA providing a coincidence event rate of 60–100 counts per second.

Three sets of data were taken with different angle settings for the decay stacks and data were obtained for 18 different angles between 25° and 155°. The actual angles at which data were taken for the different runs are given in Table I.

EXPERIMENTAL RESULTS AND DATA ANALYSIS

General features of the data

Two-dimensional spectra from ^{28}Si$(\alpha,\alpha'\alpha)$ and ^{28}Si$(\alpha,\alpha'p)$ reactions obtained at 55° (decay detector) are shown in Fig. 2 after subtraction of the accidental coincidences. Several loci which correspond to specific final states of the residual nuclei are apparent. The strong decay channels are alpha decay to the 0^+ ground state (α_0) and to the 2^+, 1.37 MeV state (α_1) of ^{24}Mg, and proton decay to the $\frac{5}{2}^+$ ground state (p_0) and to the $\frac{1}{2}^+$, 0.84 MeV and $\frac{3}{2}^+$, 1.01 MeV state ($p_{1,2}$) of ^{27}Al. The 0.84 MeV and 1.01 MeV levels were not resolved.

Projections of events lying along the loci for these states on the alpha axis are shown in Fig. 3 for decay angles of 25° and 155°. Resonant structures can be seen with very little continuum in the alpha and proton spectra taken at 155°. In the 25° proton decay spectra, however, there appears to be a significant continuum. The alpha decay spectra at 25° exhibit at most a small continuum. The continuum in the proton spectra may come from knockout where an incident alpha particle knocks out a proton in the nucleus, leaving it in a hole state, as discussed later.

A singles α' spectrum is shown in Fig. 4(a). An α' spectrum of events in coincidence with decay alpha particles or protons, obtained by summing the decay spectra (after subtraction of accidental coincidences) with the appropriate $\sin\theta$ weighting factor and normalized by the solid angle subtended by the decay detector is shown in Fig. 4(b). The data in Figs. 4(a) and (b) were taken simultaneously, and the relative normalizations are dependent only on the singles step down ratio, not on charge, target thickness, or dead time. In the singles spectrum, there exists a broad, strong peak at an excitation energy around 17.5 MeV which was reported by Lui *et al.*[5] to contain significant monopole and quadrupole strength. A relatively narrow component of this peak dominates the coincidence spectrum below $E_x = 20$ MeV with a peak to continuum ratio $> 3{:}1$. The integrated cross section for the strong peak (primarily 0^+) is about 87% of the cross section for the same peak in the singles spectrum. As the threshold for neutron decay is 17.2 MeV, the balance of decay of this state could be neutron decay. The continuum in Fig. 4(b) is considerably lower than that in Fig. 4(a), even below the neutron threshold, suggesting experimental (slit scattering) contributions to the spectrum. Below the neutron threshold the integrated cross section in the singles spectrum is about twice that which can be accounted for from the coincidence data. As partial confirmation of the origin of this discrepancy, in data taken on ^{24}Mg during the same run period but with improved optics, the sum of the decay data did reproduce the singles spectrum below the neutron threshold. The fine structure in the individual decay spectra in Fig. 3 does not correspond well to that in the singles spectrum; however, that in the summed coincidence spectrum does correspond to the structure in the singles spectra.

To obtain angular correlation functions, the coincidence spectra were divided into several excitation energy bins roughly corresponding to the structure in the singles spectrum. In Figs. 5 and 6, the angular correlations for the α_0 and α_1 decay channels, respectively, are shown for each energy bin, and Fig. 7 shows the correlations for the entire region from 15.5 to 26 MeV. The error bars shown on the data points correspond to the statistical error after subtraction of accidental coincidences. The angular correlations for α_1 decay in the lowest excitation energy region ($E_x = 15.5$–16.7 MeV) were not obtained because the kinematics locus of the α_1 decay in this region crosses the alpha particle threshold in the decay detectors.

The angular correlations for α_0 and α_1 decay summed over the entire region are almost symmetric about 90°. This suggests that contributions from quasifree scattering are small. In the angular correlations for some of the individual energy bins, however, there is a small forward-backward asymmetry. If the finite solid angle of the decay detector is not taken into account, the angular correlation of the α_0 decay from the GQR [in plane-wave Born approximation (PBWA)] should be proportional to $[P_2(\cos\theta)]^2$, where $P_2(\cos\theta)$ is the Legendre polynomial.

The experimental angular correlations of the α_0 decay show this $E2$-like pattern with a relatively large zero offset. This suggests that the main contributions to the α_0 decay come from $E0$ and $E2$ (although, over the region covered, higher multipolarities cannot be ruled out—this is discussed later).

It is interesting to note that the individual correlations in fact do have some forward backward asymmetry and that the cross section around 90° is sometimes higher and sometimes lower relative to the forward peak than would

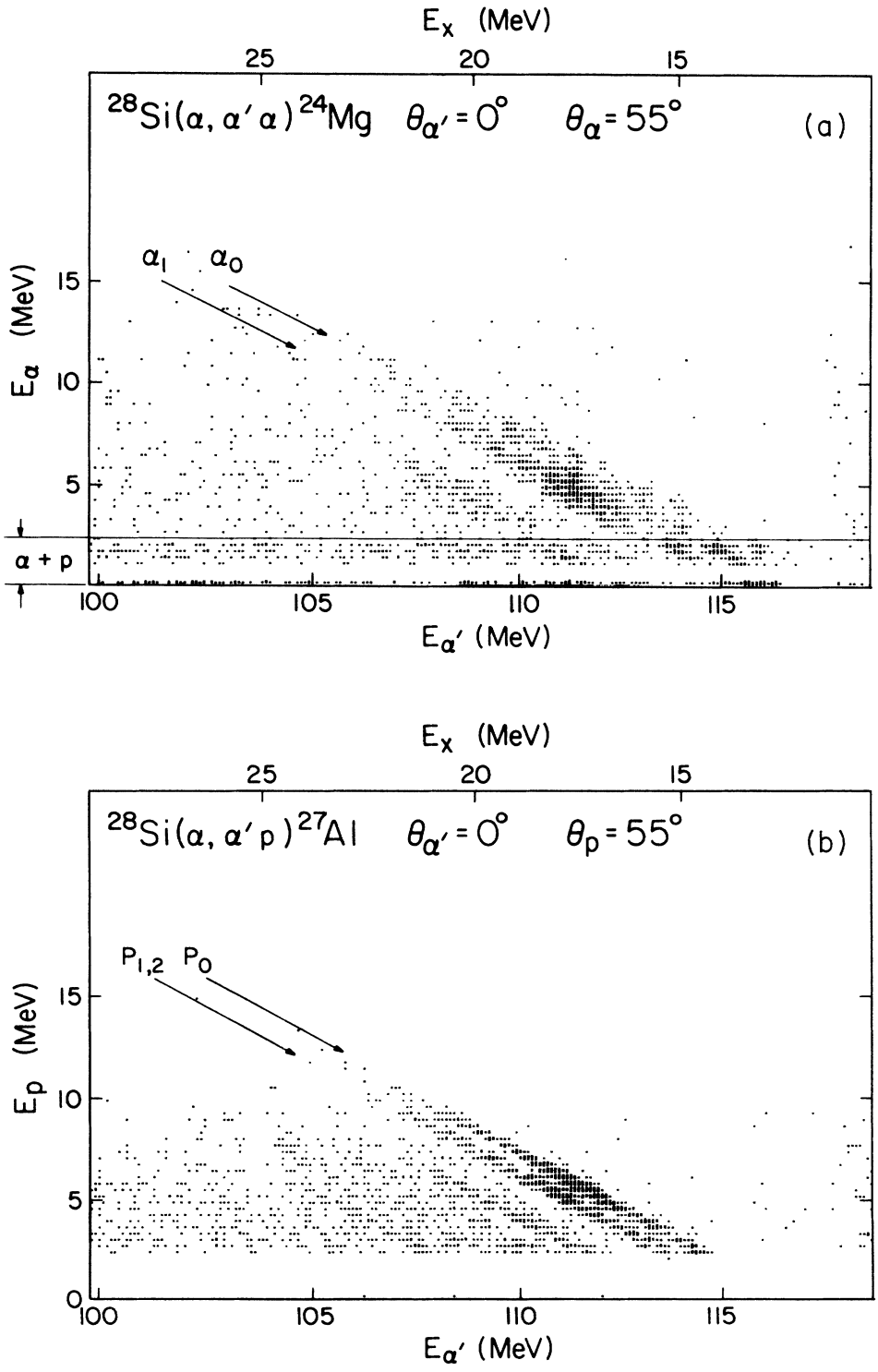

FIG. 2. True coincidence spectra of ^{28}Si($\alpha,\alpha'\alpha$)^{24}Mg and ^{28}Si($\alpha,\alpha'p$)^{27}Al reactions. In the low-energy part ($E_\alpha \leq 2.6$ MeV) of the ^{28}Si($\alpha,\alpha'\alpha$) spectrum, α and p are not separated. Accidental coincidences have been subtracted.

be true for a pure $[P_2(\cos\theta)]^2$. The lower cross section at 90° suggests that there may exist interference between $E0$ and $E2$ decays in the overlapping resonance region as might be expected from the results of Lui *et al.*[5] The forward-backward asymmetry may result from interference with a multipole of opposite parity.[15]

The α_1 angular correlations also show the $E2$-like pattern except in the 16.7–17.2 MeV region, but with a larger offset than the α_0 decay. There are three components in alpha decay between two 2^+ states, corresponding to $l=j=0$, 2, and 4, where l and j are orbital and total angular momenta of the decaying alpha particle. The $l=j=0$ component has the same isotropic correlation as for $E0$ decay and cannot be distinguished from it. In a previous study[15] of decay of the ^{28}Si GQR, this component was found to be small. If that is true here, the large isotropic component of the correlation would imply a large $E0$ strength in the α_1 channel.

At forward angles, the proton spectrum contains a significant continuum contribution which results in a strong forward-backward asymmetry in the angular correlations. Processes which would be forward peaked include pickup-breakup reactions (such as $^{28}\mathrm{Si}+\alpha \rightarrow {}^{27}\mathrm{Al}+{}^{5}\mathrm{Li}\rightarrow {}^{27}\mathrm{Al}+\alpha+p$) (see Ref. 17) and quasifree knockout processes. From the kinematics of the proton pickup-breakup processes, such contributions would

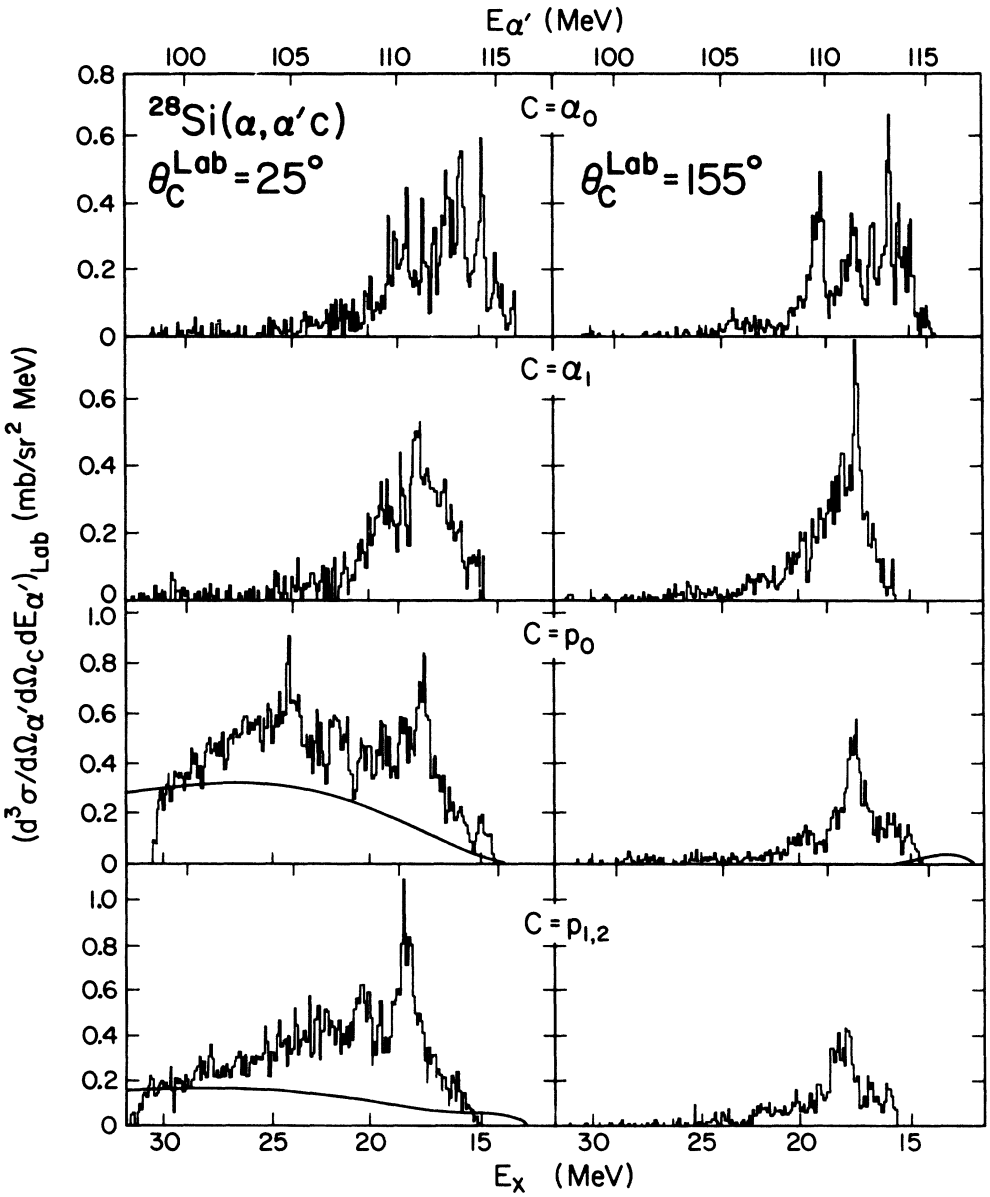

FIG. 3. Spectrum of alpha particles measured at 0° in coincidence with decay to the ground (α_0) and first excited (α_1) states of ^{24}Mg and with decay to the ground (p_0) and ($p_{1,2}$) first two excited states of ^{27}Al at the lab decay angles 25° and 155°. The lines in the p_0 and $p_{1,2}$ spectra are calculations of proton knockout.

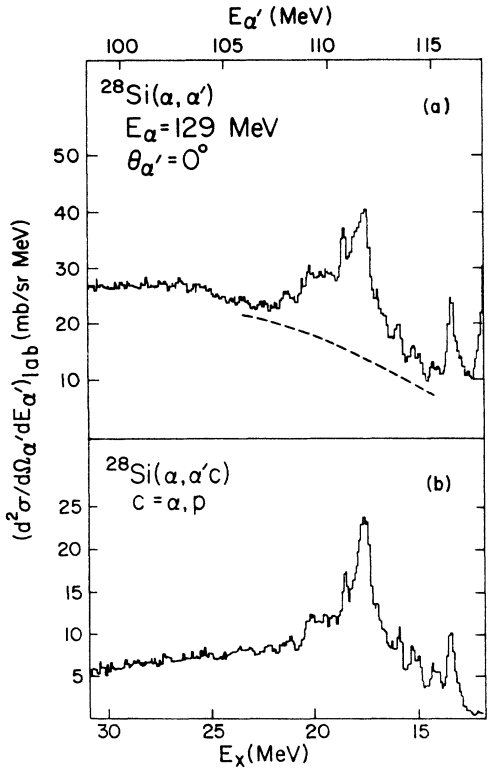

FIG. 4. (a) $^{28}Si(\alpha,\alpha')$ singles spectrum taken at 0° during the first of the three runs listed in Table I. (b) α' spectrum corresponding to all decay particles (after subtraction of accidentals) summed with $\sin\theta$ weighting for same run as part (a). See the text.

occur only in the region corresponding to excitation energies higher than 24.3 MeV ($E'_\alpha < 104.7$ MeV), whereas the observed continuum continues down to 15 MeV excitation. Because the opening angle of the spectrograph was ±2.1°, the kinematics for two-body scattering suggest that low-energy protons from quasifree alpha-proton scattering could be present in the proton spectra at forward angles. On the other hand, low-energy alpha particles from quasifree alpha-alpha scattering would be emitted near 90° with very low energy ($\leq$200 keV for free scattering).

To estimate the proton knockout contribution, plane-wave Born approximation (PWBA) calculations[18] have been performed. These are shown as solid lines in Fig. 3 for the p_0 and $p_{1,2}$ decay channels. It is apparent that the shapes of the calculated cross sections are a plausible representation of the continuum contribution. These results were obtained with a large radial cutoff (6 fm) in the integration, and the calculated cross sections were normalized to the data.

In Figs. 8 and 9, the angular correlations for the proton decay channels are shown after subtraction of the knockout contributions. The correlation for the entire region is shown in Fig. 7. In the lower excitation energy region ($E_x < 18.4$ MeV), the angular correlations are almost symmetrical about 90° in the p_0 decay channel and do not show a strong forward-backward asymmetry in the $p_{1,2}$ decay channels. In the higher excitation energy region, however, a strong enhancement of the cross section exists at forward angles (less than 40°–50°) and becomes larger as excitation energy increases. Thus, even with a knockout contribution subtracted, an enhancement of the cross sections at forward angles remains. It is unlikely that the remaining asymmetry is due to an incomplete model of the knockout (as can be seen from the proton spectrum in Fig. 3), but might be due to interference between the quasifree process and other processes[19] or interference between states of odd and even parity. Other works looking only at GQR decay have explored the possible sources of such asymmetries at length,[19,20] and this was not pursued further in this work.

In order to obtain the cross sections for alpha and proton decay into each channel, the angular correlation data were fitted with Legendre polynomials using a least-square fitting technique[21] and integrated. A few data points at forward angles (less than 40°–50°) in the proton

TABLE II. Decay strength obtained from the angular correlations for α_0 decay.

E_x (MeV)	$E0$ (% EWSR)	$E2$ (% EWSR)	$(\delta_2-\delta_0)$ (deg)	$E3$ (% EWSR)	χ^2
15.5–16.0	0.99±0.20	0.45±0.19	90	0±0.014	1.3
16.0–16.7	0.79±0.21	0.65±0.31	88	0.015±0.064	3.4
16.7–17.2	0.74±0.18	0.25±0.21	102	0±0.072	1.6
17.2–18.4	2.5±0.2	0.72±0.51	98	0±0.019	2.2
18.4–19.1	0.89±0.21	0.49±0.08	92	0.095±0.001	1.6
19.1–20.1	1.4±0.2	0.54±0.11	70	0.035±0.020	1.5
20.1–21.2	1.2±0.2	0.03±0.03	85	0±0.004	2.3
21.2–22.5	0.74±0.22	0.13±0.06	90	0.12±0.02	2.1
Total					
15.5–22.5	9.2±1.6	3.3 ±1.5		0.27±0.22	
15.5–22.5	10.3[a]	3.6[a]	88[a]		2.9[a]

[a]Fitting the angular correlation for the entire energy region.

angular correlations were omitted from the fits, because in that angular region, nonresonant components appear to exist. Decay particles with energies below 2.6 MeV were excluded because alpha and proton decay could not be distinguished in this energy region; this corresponded to 12% of the decay.

These decay cross sections are plotted as a fraction of the singles giant resonance cross section in Fig. 10(a). The singles giant resonance cross section was obtained from the spectrum in Fig. 4(a) by subtracting the empirical background indicated by the dashed line. Below the neutron threshold (17.2 MeV) where the decay should proceed predominantly through p and α decay, approximately 100% of the decay is accounted for in these experiments, about 60% α and 40% p decay, if the particles below 2.6 MeV are assumed to be α. In the region of the strongest concentration of GR strength (17–19 MeV), alpha particle decay decreases relative to the proton decay.

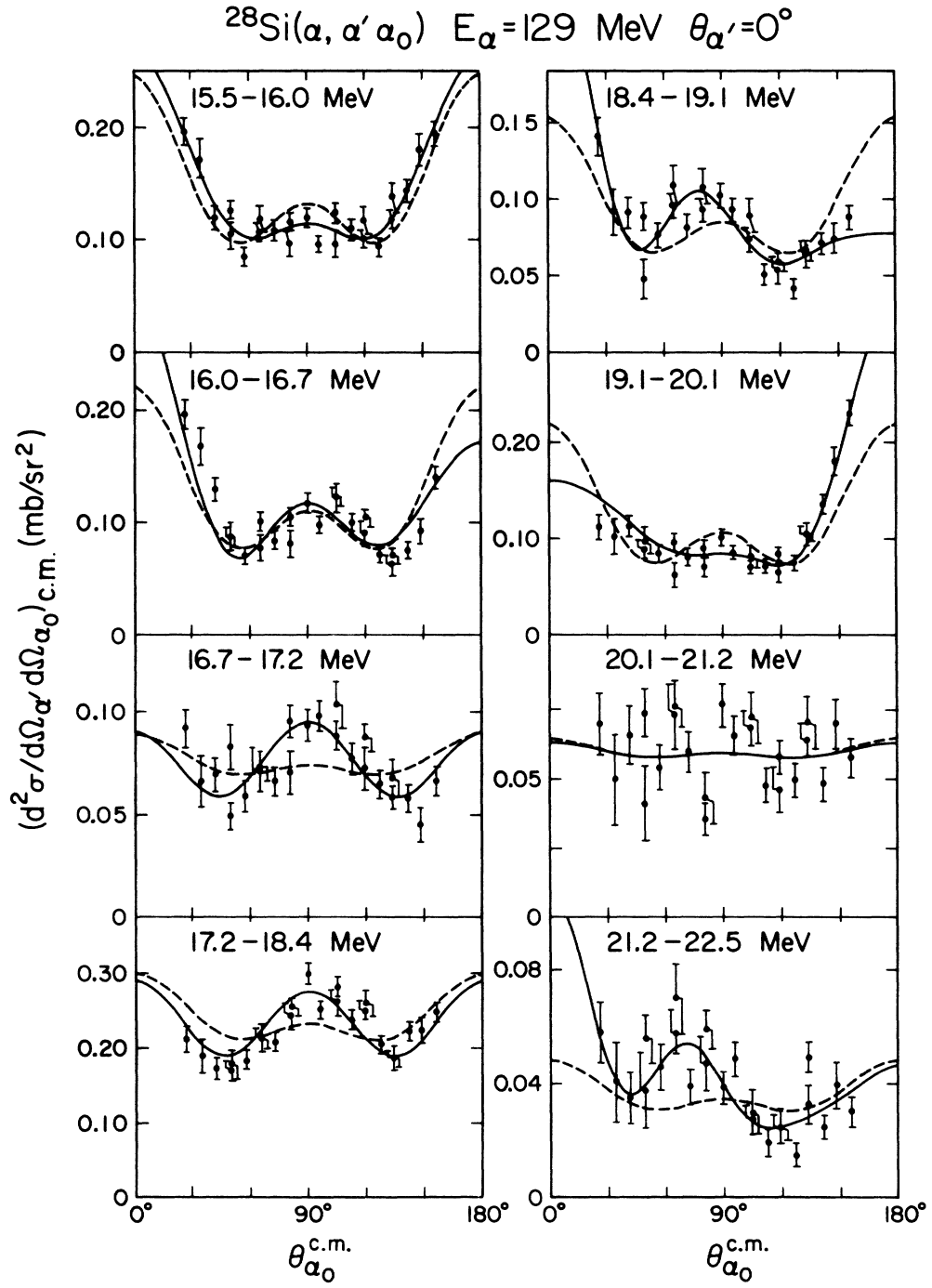

FIG. 5. Angular correlations for α_0 decay from the indicated excitation energy regions of ^{28}Si. Solid (dashed) lines are angular correlations calculated with coherent (incoherent) mixing of decay amplitudes with parameters as listed in Table II.

TABLE III. Decay strength obtained from the angular correlations for α_1 decay. The two values given for the 17.2–18.4 MeV region (and the total) represent essentially equal quality fits.

E_x (MeV)	$L=0$[a] (% EWSR)	$L=2$ ($l=j=2$) (% EWSR)	$\delta_2-\delta_0$ (deg)	$L=2$ ($l=j=4$) (% EWSR)	$\delta_2-\delta_0$ (deg)	χ^2
16.7–17.2	0.45±0.18	0.37±0.21	102	0.99±0.21	102	2.1
17.2–18.4	4.9±0.2	2.0±0.5	270			4.6
	5.4±0.2			1.1±0.5	98	4.8
18.4–19.1	1.8±0.2			0.69±0.08	92	1.4
19.1–20.1	1.8±0.2			1.1±0.1	80	2.2
20.1–21.2	1.0±0.2			1.0±0.1	90	1.7
21.2–22.5	0.72±0.22			0.70±0.06	95	0.8
Total						
16.7–22.5	10.7±1.2	2.4±0.7		4.5±0.6		
		0.37±0.21		5.6±1.1		
16.7–22.5	15.1[b]			1.5[b]	88[b]	3.3[b]

[a] $E2$ ($l=j=0$) strength is not distinguished, but neglectable (see the text).
[b] Fitting the angular correlation for the entire energy region.

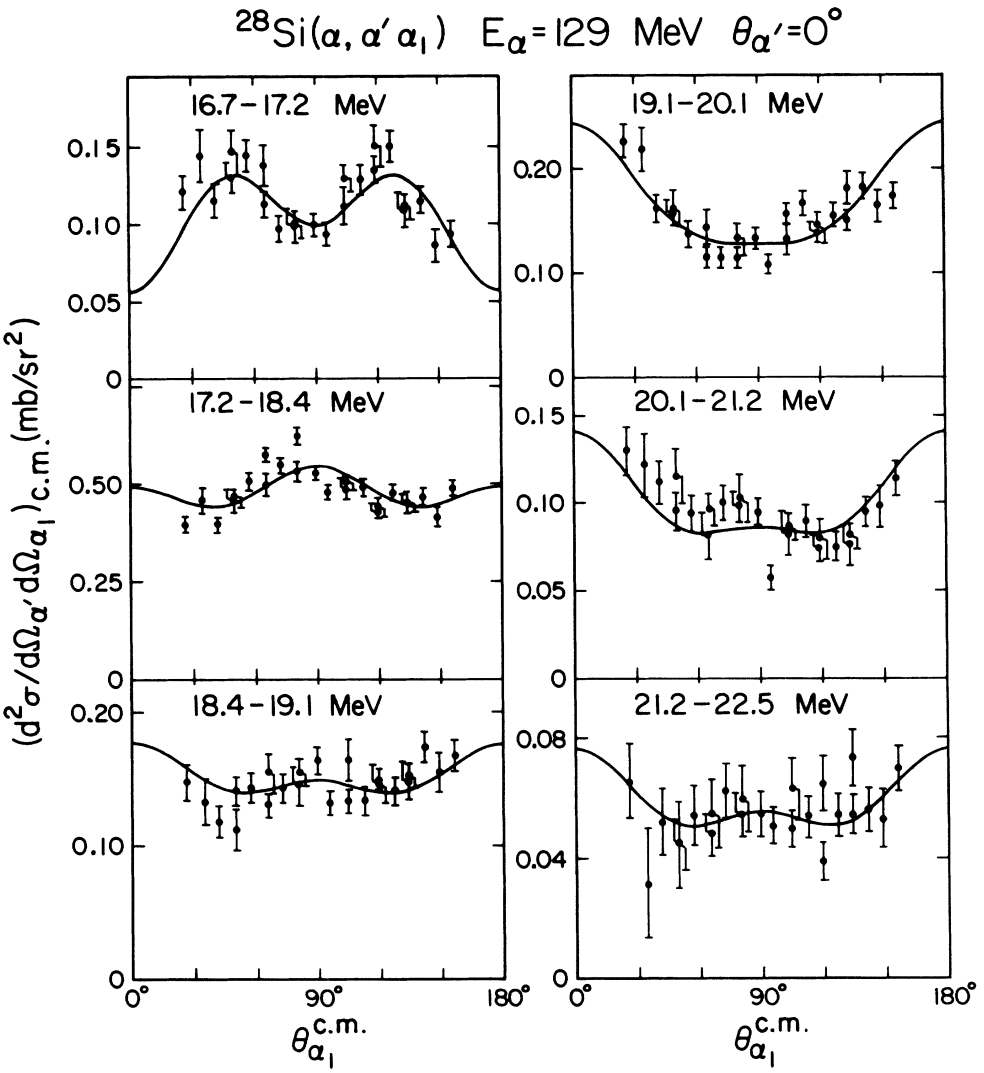

FIG. 6. Angular correlations for α_1 decay from the indicated excitation energy regions of ^{28}Si. Solid lines are angular correlations calculated with coherent mixing of decay amplitudes with parameters as listed in Table III.

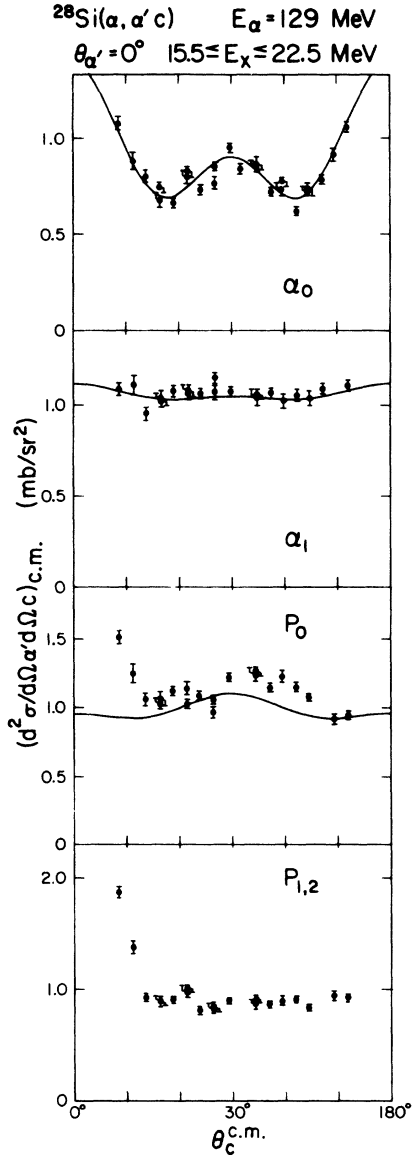

FIG. 7. Angular correlations for α_0, α_1, p_0, and $p_{1,2}$ decay from the giant resonance region of ^{28}Si. For α_1 decay, the data correspond to $E_x=16.7-22.5$ MeV (see the text). Solid lines are calculated angular correlation functions with coherent mixing for α_0 and α_1 decay and incoherent mixing for p_0 decay.

Above the GR peak (>20 MeV), alpha and proton decays are comparable, and the sum considerably exceeds the singles GR yield, no doubt reflecting decay of the continuum. Unfortunately, the presence of slit scattering in the singles spectrum prevents extraction of meaningful absolute decay branches above the GR peak.

For comparison, the branching ratios of statistical decays, estimated with a Hauser-Feshbach calculation using the nuclear evaporation code (with parity conservation) CASCADE,[22] are shown for the decay from the GMR and GQR in Figs. 10(b) and 10(c), respectively. If the giant resonances are assumed to decay statistically, the branching ratio of neutron decay is 10–15 % at $E_x>18$ MeV, as shown in Figs. 10(b) and 10(c). This is also approximately the amount needed to explain the singles/coincidence difference for the strong 0^+ peak. The predicted ratio of alpha to proton decay is almost 1:1, the same as previously observed in the GQR decay.[15]

Angular correlation analysis and sum rules

In order to obtain the strength of the GMR, GQR, and other multipoles present, angular correlation functions were calculated and fit to the data. The angular correlation for a particle decay from an isolated resonant state with a spin I_r and z component m_r can be written[23] as

$$W(\hat{p}_b)=\sum_{m_b,m_r}|g(I_r m_r\rightarrow I m\hat{p}_b m_b)T_{m_r}|^2 \quad (1)$$

where,

$$g(I_r m_r\rightarrow I m\hat{p}_b m_b)=\sum_{lj}\langle lm_l s_b m_b|jm_j\rangle\langle Im_j m_j|I_r m_r\rangle \times Y_l^{m_l}(\hat{p}_b)g(I_r\rightarrow Ilj) \quad (2)$$

and $g(I_r\rightarrow Ilj)$ is a decay amplitude which has a phase as the phase shift of the nonresonant scattering in the decay channel and $|g(I_r\rightarrow Ilj)|^2$ gives a partial decay width $G(I_r\rightarrow Ilj)$. The spin and z component of the decay particle (residual nucleus) are given by s_b and m_b (I and m), respectively, and l and j (m_l and m_j) are orbital and total angular momentum (z component) of the decay particle, respectively. The decay particle is emitted to the direction p_b. T_{m_r} is the m-substate population of the resonant state. For alpha inelastic scattering on a spin-zero target, T_{m_r} is given by a transition matrix which can be calculated in the distorted-wave Born approximation (DWBA).[24] If resonances are overlapping, the decay from different resonant states can interfere coherently.

DWBA calculations to obtain the m-substate population were carried out with the computer code DWUCK4;[25] the usual form factors were used (for a detailed discussion of form factors used for the $L=0$ mode and the optical model parameters, see Ref. 5). The finite solid angles of the spectrometer and the decay detectors were taken into account in the calculation of the angular correlation. The correction for the finite opening angle of the spectrometer detector was important, as the correlation was somewhat washed out because the recoil angle of the target nucleus is large even for a small α' angle. For example, the recoil angle is 28° for $E_x=15$ MeV and $\Theta(\alpha')=2°$. Therefore, the angular correlation pattern for $L\geq 2$ shifts considerably over the angular opening of the spectrometer, washing out the pattern somewhat.

α_0 decay

The experimental angular correlations were fitted with a coherent mixture of $E2$ and $E0$. Where small asymmetries were present, some $E3$ admixture was added to the calculation. In Fig. 5, the best-fit results of the calculations with the coherent mixing are shown as solid lines. Parameters obtained from the χ^2 fitting are listed in Table II. δ_L is the phase of the complex coefficient

$|g(I_r \rightarrow Ilj)|$ in Eq. (2), and the fraction of the EWSR is obtained from $|g(I_r \rightarrow Ilj)|^2$ as explained above. The procedure followed in the fits is described below. As the angular correlation is not a linear function of the parameters [the strength and phase of $g(I_r \rightarrow Ilj)$], the angular correlations were calculated at many points in the parameter space, and the parameter set which minimized χ^2 was obtained. An example of the "fitting" procedure is shown for the 17.2–18.4 MeV data in Fig. 11. First, strengths of 2.7% of the $E0$ EWSR and 0.37% of the $E2$ EWSR were obtained from a calculation assuming incoherent mixing. Angular correlations were then calculated with the coherent mixing for a wide range of parameters around these values and wide range of phase parameters, with coarse steps of parameter values. In Fig. 11, χ^2 for the fits are shown, for example, for $E2$ strengths of 0.28%, 0.69%, and 1.25% of the EWSR, respectively, with several $E0$ strengths from 0.67% to

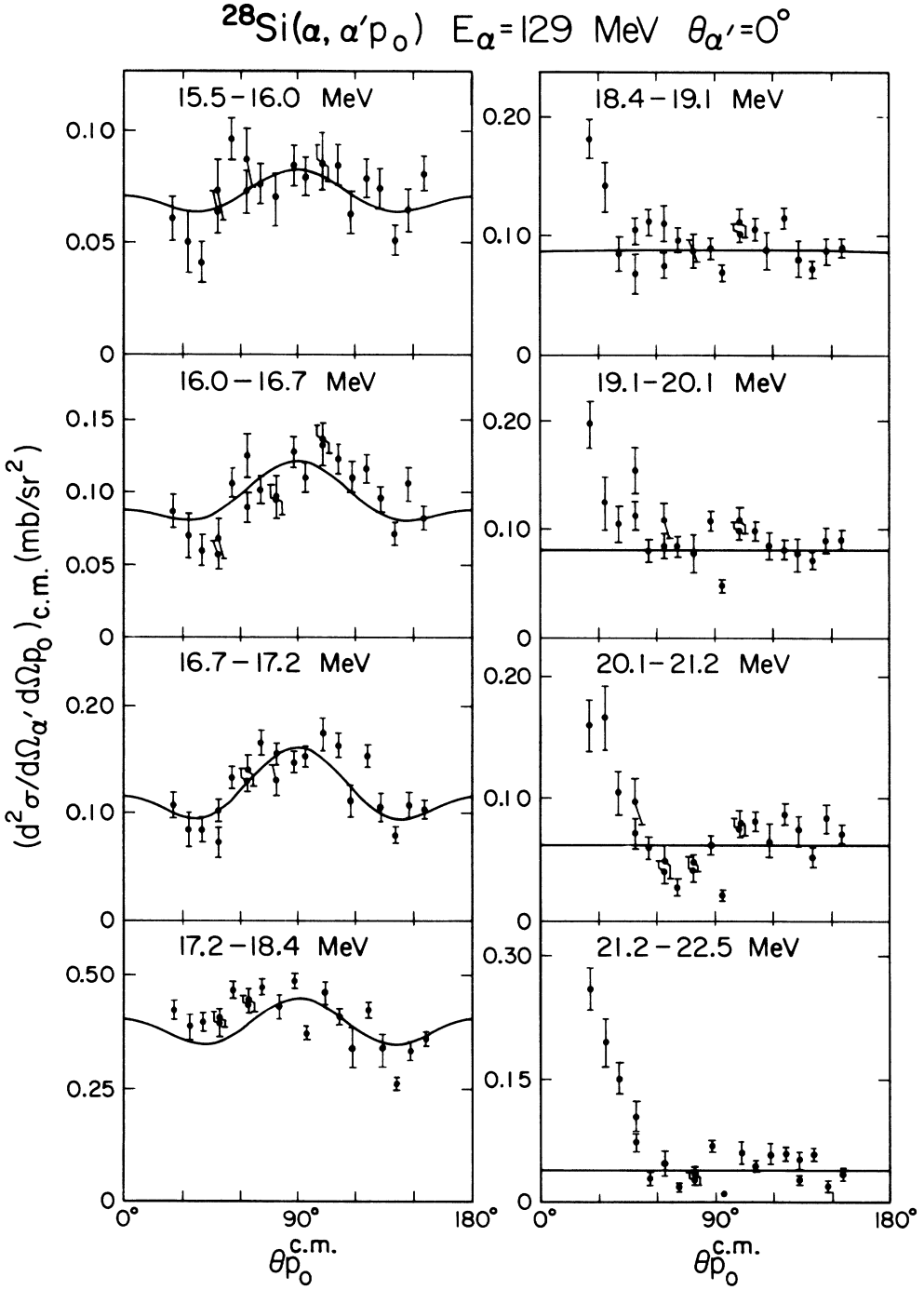

FIG. 8. Angular correlations for p_0 decay from the indicated excitation energy regions of ^{28}Si. Solid lines are calculated angular correlations with incoherent mixing of decay amplitudes with parameters as listed in Table IV.

4.66% of the EWSR and phase parameters $(\delta_2-\delta_0)$ from 0° to 350°. There are two minima in the χ^2 curve (around 100° and 250°) with about the same value. This phase ambiguity is normal and either value can be used. The best fit parameters were then obtained by varying the parameters in fine steps around the values near one minimum.

The sensitivity of χ^2 to each parameter is also shown in Fig. 11, while Fig. 12 shows the extent to which the angular correlation can be changed by varying the parameters. The uncertainty in each parameter has been estimated from these variations taking into account the statistical errors and variations which could be caused by differing gates for each decay channel (α_0 vs α_1, etc.).

The forward-backward asymmetry present in some of the correlations was reproduced well by including a small amount of $E3$ strength, consistent with the study of ^{28}Si GQR decay.[15] No contributions from $E4$ were necessary

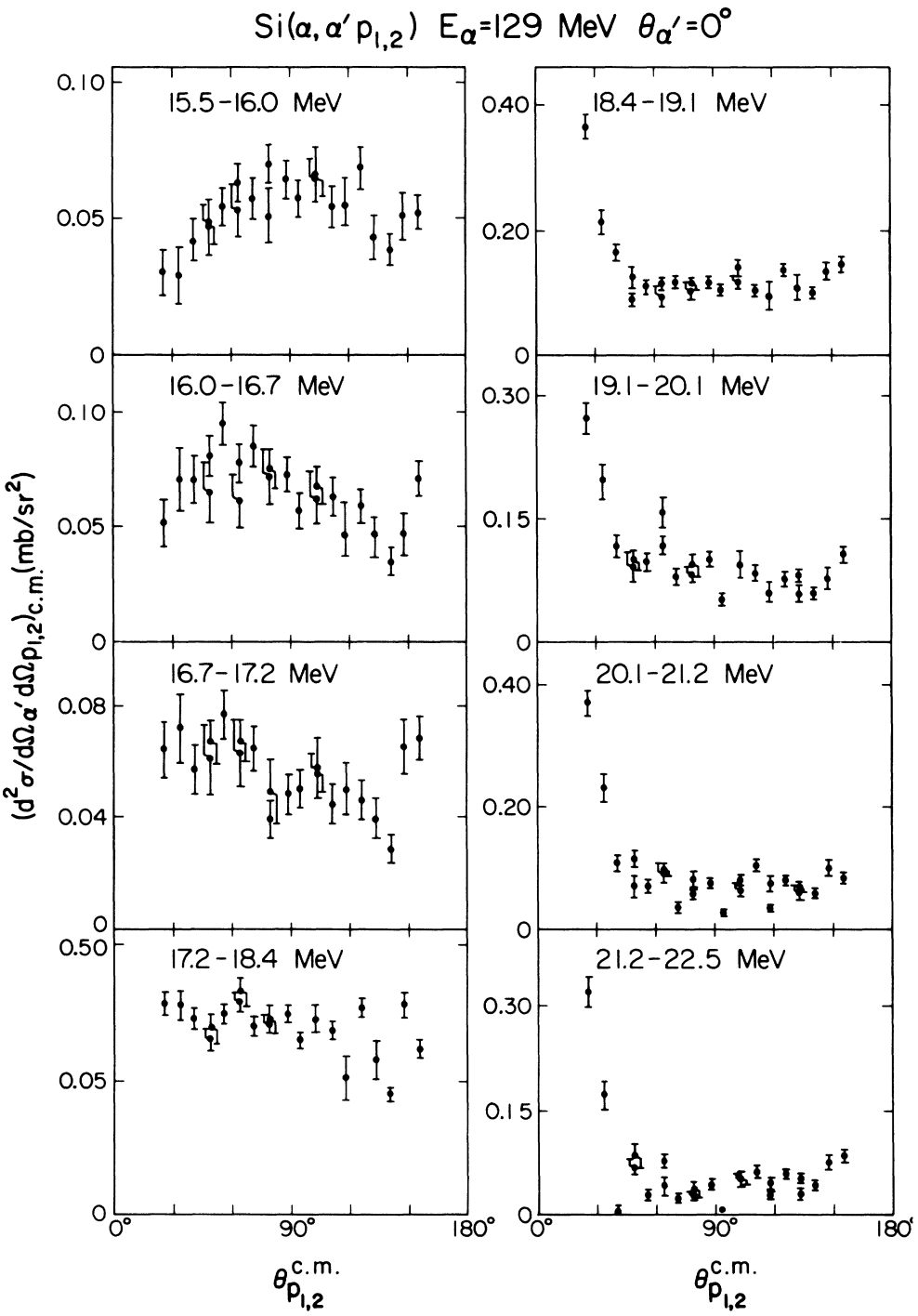

FIG. 9. Angular correlations for $p_{1,2}$ decay from the indicated excitation energy regions of ^{28}Si.

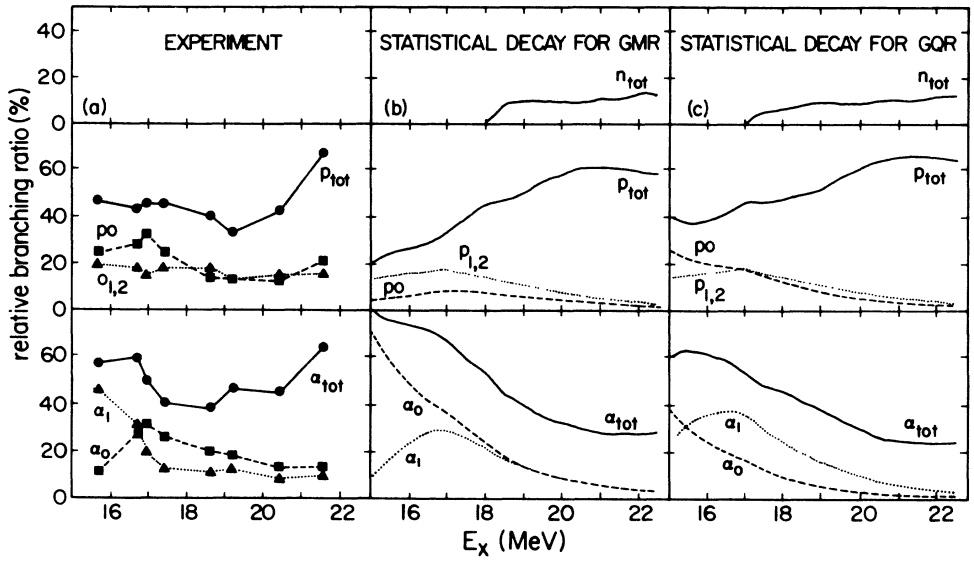

FIG. 10. (a) Experimental alpha and proton decay branching ratios of ^{28}Si excited to the indicated excitation energy by 129 MeV alpha particles detected at 0°. Below the $E_x = 17.2$ MeV neutron threshold, $\alpha_{tot} + p_{tot}$ was assumed to be 100% of the decay. Above 17.2 MeV, only relative branching ratios could be determined (see the text). (b) and (c) are alpha and proton branching ratios for the GMR and GQR, respectively, predicted for statistical decay with Hauser-Feshbach calculations.

to fit the data, in contrast with the singles results.[5] In general, fits from the coherent mixing calculations resulted in a χ^2 lower by a factor of 2–3 than for incoherent calculations. In Figs. 13 and 14, respectively, the distributions of the $E0$ and $E2$ strength and the phase difference $(\delta_2 - \delta_0)$ are shown. It is interesting to note that the strength distributions of the $E0$ and $E2$ and even the phase differences show a gross structure.

Other decay channels

Only the α_0 channel, decay of a spin-zero particle to a spin-zero final state, has a unique l wave in the decay of the $E2$. In the other channels, decay can proceed through at least two l waves, and extraction of meaningful parameters is more ambiguous. Results of an analysis of these channels is described below. In general, the same fitting procedures were applied as in the α_0 case; however, it must be recognized that a number of assumptions which may be plausible but not rigorously defensible must be made to draw significant conclusions.

In the α_1 decay channel $(0^+, 2^+ \rightarrow 2^+)$, $l = j = 0$, 2, and 4 can contribute to the decay. The $l = j = 0$ component of the $E2$ decay was neglected for simplicity because the GQR decay study of ^{28}Si (Ref. 15) has shown that this contribution was very small. In Fig. 6, the results of the

TABLE IV. Decay strength obtained from the angular correlations for p_0 decay (incoherent mixing).

E_x (MeV)	$E0$[a] (% EWSR)	$E2$ $(l=2, j=\frac{5}{2})$ (% EWSR)	$E2$ $(l=2, k=\frac{3}{2})$ (% EWSR)
15.5–16.0	0.45±0.10	0.34±0.23	0.09±0.20
16.0–16.7	0.47±0.13	0.61±0.28	0.41±0.24
16.7–17.2	0.39±0.12	1.2±0.3	0.48±0.26
17.2–18.4	3.6±0.6	2.6±0.8	0.26±0.51
18.4–19.1	1.4±0.3	0.02±0.20	
19.1–20.1	1.4±0.3		
20.1–21.2	1.3±0.5		
21.2–22.5	0.97±0.33		
Total			
15.5–22.5	10.0±2.4	4.8±1.8	1.2±1.2
15.5–22.5	11.4[b]	2.8[b]	1.8[b]

[a] $E2$ $(l=0, j=\frac{1}{2})$ strength was not distinguished (see the text).

[b] Fitting the angular correlation for the entire energy region.

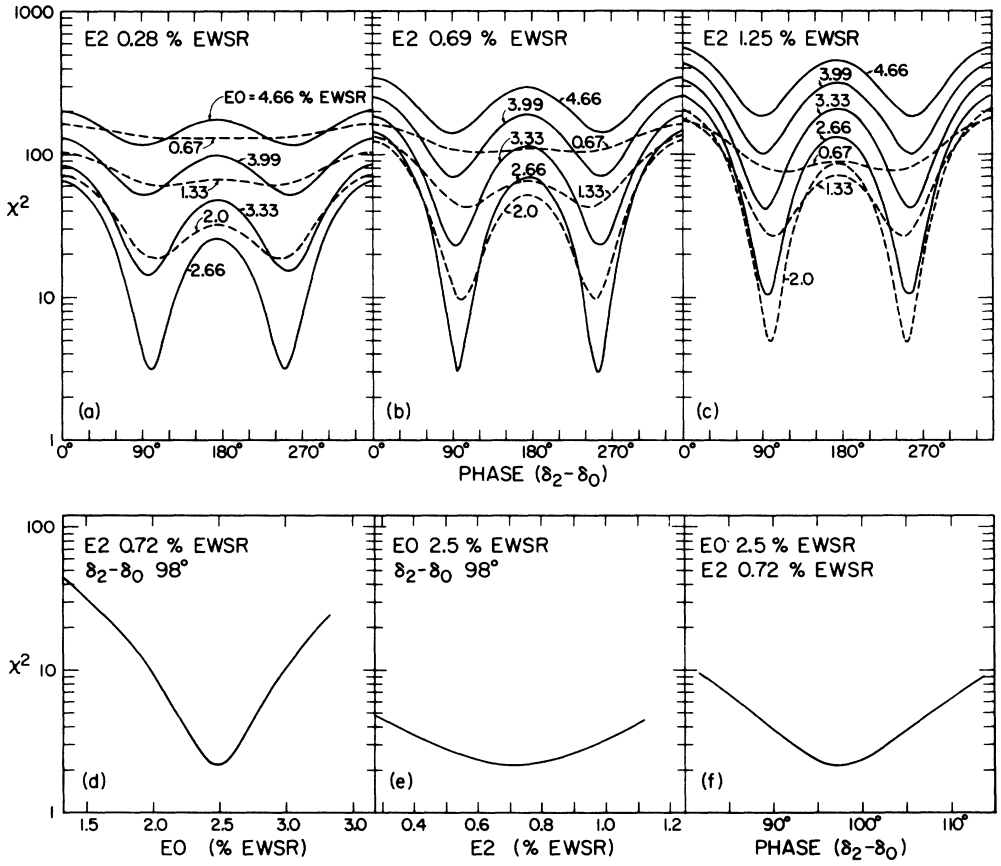

FIG. 11. χ^2 as a function of phase angle for fits to the α_0 angular correlation data in the $E_x = 17.2-18.4$ MeV region using a coherent mixing calculation for different values of $E0$ strength (0.67–4.66 % EWSR). (a), (b), and (c) show the results for three values of $E2$ strength: 0.28%, 0.69%, and 1.25% EWSR, respectively. (d), (e), and (f) show χ^2 for fits as a function of the $E0$ strength, $E2$ strength and phase $\delta_2 - \delta_0$, respectively, around the best fit parameters.

TABLE V. $E2$ decay strength and branching ratios from ^{28}Si$(\alpha,\alpha c)$ experiments.

Decay channel	E_x (MeV)	Present study[a] (% EWSR)	(BR)	^{28}Si$(\alpha,\alpha c)$[b] (% EWSR)	(BR)
α_0	15.5–18.4	2.1±1.2			
	18.4–22.5	1.2±0.3			
	15.5–22.5	3.3±1.5	8.0±3.7 %		
	16.9–24.8			$3.4^{+1.1}_{-0.8}$	11±2 %
α_1	16.7–22.5	6.5±1.4	18±4 %[c]		
	16.9–24.8			$8.7^{+2.4}_{-1.7}$	28±3 %
p_0	15.5–22.5	(7.0±1.7)[d]	d		
	16.9–24.8			$6.8^{+2.0}_{-1.4}$	22±3 %
$p_{1,2}$	15.5–22.5	(6.4±1.5)[d]	d		
	16.9–24.8			$6.2^{+1.9}_{-1.4}$	20±3 %

[a]Branching ratio was obtained assuming an $E2$ strength of 32±6 % EWSR in the excitation region 15.3–23.0 MeV (Ref. 5).
[b]Branching ratio (BR) comes from Ref. 15 in which the 15.4–24.8 MeV excitation region was studied. Decay strength was obtained using 31^{+8}_{-5}% EWSR in the 16.9–24.8 MeV region for GQR from Ref. 31 and the branching ratio 11±2 % for α_0 decay, 28±3 % for α_1 decay, 22±3 % for p_0 decay, and 20±3 % for $p_{1,2}$ decay from Ref. 15.
[c]$E2$ strength assumed to be 29±5 % EWSR in the $E_x = 16.9-23.0$ MeV region from Ref. 5.
[d]The p_0 and $p_{1,2}$ branching ratios in Ref. 15 were used to obtain % EWSR (see the text) assuming total $E2$ strength from Ref. 5.

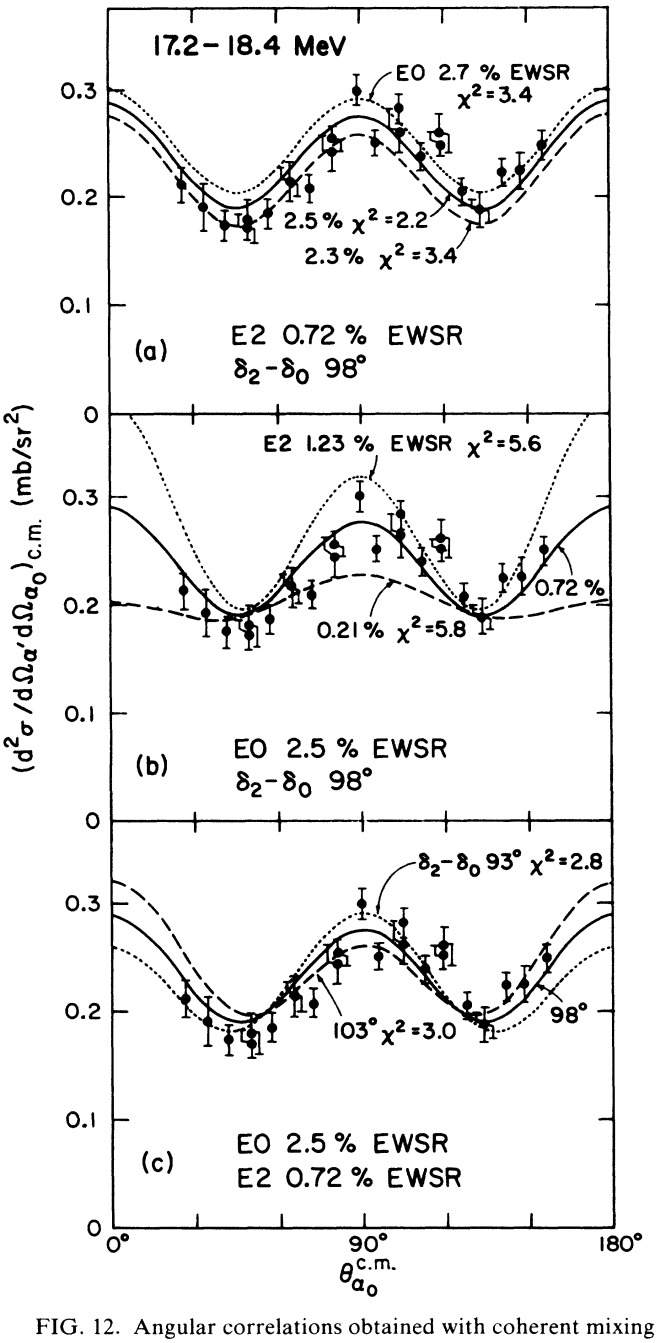

FIG. 12. Angular correlations obtained with coherent mixing for the $E_x=17.2-18.4$ MeV α_0 data for parameters around the best fitting parameter, changing, respectively, (a) $E0$ strength from 2.3% to 2.7% EWSR, (b) $E2$ strength from 0.21% to 1.23% EWSR, and (c) phase $(\delta_2-\delta_0)$ from 93° to 103° each holding the other parameters fixed at the indicated values.

angular correlation calculations for the α_1 decay are shown as solid lines. In contrast with the α_0 decay channel, the experimental α_1 angular correlations did not show distinct asymmetries, and $E3$ was not included in the fit. The strengths and phases obtained are listed in Table III. Best fits were obtained from coherent mixing of the $E0$ and $E2$ strength with almost the same phase difference $(\delta_2-\delta_0)$ as in the α_0 decay for each energy bin. In the 17.2–18.4 MeV region, two different sets of parameters gave almost equally good fits, as listed in the table. One has an $l=j=4$ component from the GQR decay with the same phase difference (98°) as in the α_0 decay and the other an $l=j=2$ component with an almost opposite phase difference of 270° ($=-90°$), which is physically possible if the wave function with $l=j=2$ has the opposite sign. The shape of the angular correlation in the 16.7–17.2 MeV region is very different from that expected for $E2$ decay and could not be reproduced in the calculations by coherent mixing of $E0$ and either $l=j=2$ or 4 in the $E2$. The $E0$ and $E2$ strength distributions are shown in Fig. 11.

The angular correlations of the p_0 and $p_{1,2}$ decays are even more complicated than α_1 because many decay components may compete. For example, in the p_0 decay there are components $(l,j)=(2,\frac{5}{2})$ for the $E0$ and $(0,\frac{5}{2})$, $(2,\frac{3}{2})$, $(2,\frac{5}{2})$, $(4,\frac{7}{2})$, and $(4,\frac{9}{2})$ for the $E2$. In the measured $p_{1,2}$ decay, the situation is yet more complicated because experimentally the residual states are an unresolved $\frac{1}{2}^+$, $\frac{3}{2}^+$ doublet. Therefore, coherent mixing calculations were not carried out for the proton decay. Nevertheless, several conclusions can be drawn. The p_0 angular correlations show a pattern symmetrical about 90° in the 15.5–18.4 MeV region, which favor the $(l,j)=(2,\frac{3}{2})$ and $(2,\frac{5}{2})$ components for $E2$ as well as $E0$ decay. Angular correlation calculations assuming incoherent mixing of a few components are shown in Fig. 8, and the parameters obtained are listed in Table IV. In the 18.4–22.5 MeV region, except for several data points at forward angles with enhanced cross sections, the data are isotropic.

DISCUSSION

It is interesting to compare the coincidence spectra obtained in this study (Fig. 3) with those of the ^{28}Si(α,α') coincidence experiment of Ref. 15, in which α' was measured at $\theta_{lab}=6.5°$ and therefore showed mainly $E2$ decay strength. The coincidence spectra at $\theta_{lab}=155°$ (opposite the recoil) of the present measurement have similar structure to the corresponding one of Ref. 15 (opposite the recoil), but the 17.5 MeV peak in the α_1 and p_0 decay and the structure around 18 MeV in the $p_{1,2}$ decay are enhanced in the present work. From the correlations, these are attributed primarily to $E0$ decay. In Refs. 14 and 15, the fact that the α_0 decay channel was weakly coupled to the GQR and did not reflect the strength distribution of the $E2$ in the singles spectrum, was attributed to the existence of a complicated hallway state rather than a doorway state, while a doorway state was suggested from the strong correlation of the strength distribution between the p_0, $p_{1,2}$, and α_1 decay channel and the singles spectrum. In the present measurements also the α_0 channel shows the least correspondence to the singles spectrum. The $p_{1,2}$ strength distribution is, however, a little different from the singles which shows a minimum near $E_x=18$ MeV. On the other hand, as shown in Fig. 3, the coincidence spectrum at 25° differs more from the singles than does the 155° spectrum. There is different

TABLE VI. $E0$ decay strength and branching ratios from $^{28}Si(\alpha,\alpha c)$ experiments.

Decay channel	E_x (MeV)	Present study (% EWSR)	BR[a]
α_0	15.5–22.5	9.2±1.6	18±6
α_1	16.7–22.5	10.7±1.2	24±8[b]
p_0	15.5–22.5	12.2±3.3	23±9
$p_{1,2}$	15.5–22.5	9.5±3.3	18±8

[a]Using 52±16 % for $E0$ strength in the $E_x = 15.5$–22.5 MeV region obtained from Ref. 5.
[b]Using 44±13 % for $E0$ strength in the $E_x = 16.7$–22.5 MeV region obtained from Ref. 5.

enhancement for several peaks between these angles, especially in the α_0, p_0, and $p_{1,2}$ decay and somewhat in the α_1 decay spectra. This results in asymmetry in the angular correlation which was fit, for α_0 decay, with coherent mixing of the $E3$ decay amplitude. In the proton decay channels, however, the knockout process probably contributes to the asymmetry.[19,20]

The ratios between the forward/backward peak and the 90° peak in the α_0 and α_1 angular correlation data could be fit only with coherent mixing. The necessity of using a coherent mixing calculation for angular correlations was demonstrated previously in the α_0 decay from the GQR of ^{16}O (Ref. 26), ^{24}Mg (Ref. 27), and ^{28}Si (Ref. 15) which showed forward-backward asymmetry and required mixing of opposite parity multipoles.

In the p_0 and $p_{1,2}$ decay, the fitting procedure for the angular correlation was complicated and the decay strength could not be obtained unambiguously. However, a rough estimate of the $E0$ and $E2$ decay strength of the p_0 and $p_{1,2}$ decay was obtained in the following way. The cross sections calculated with DWBA for $E0$ and $E2$ states each at $E_x \sim 18.7$ MeV with 100% of the EWSR, averaged over the finite solid angle of the spectrograph, are 81 mb/sr for $E0$ and 61 mb/sr for $E2$. From the singles experiment of Ref. 5, an $E2$ strength of 32±6 % EWSR (with the same procedure used in the present study to extract the isoscalar transition strength) was found in the $E_x = 15.3$–23.0 MeV region. Using the p_0

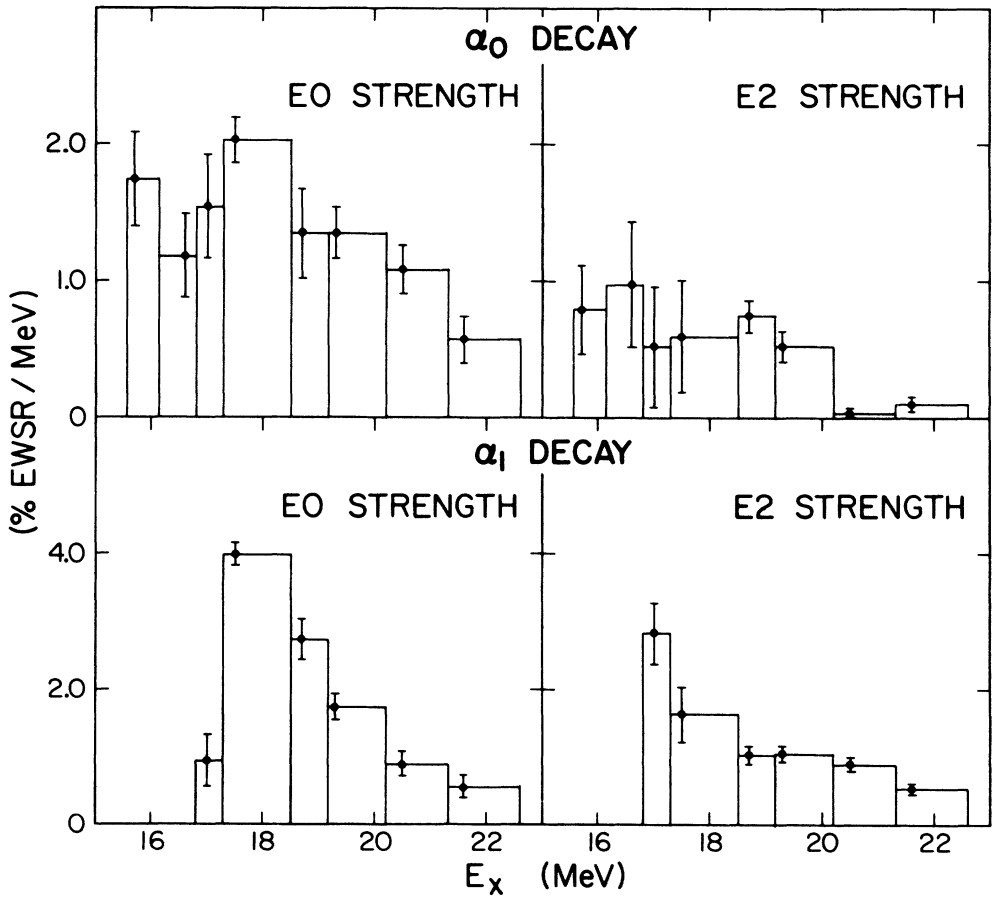

FIG. 13. $E0$ and $E2$ strength distributions obtained for α_0 and α_1 decay channels (coherent mixing).

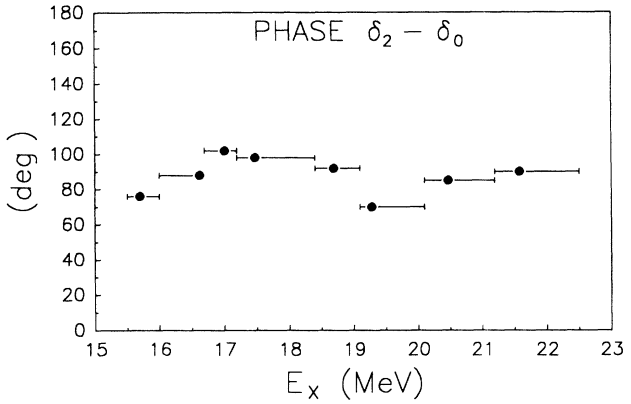

FIG. 14. Phase difference $(\delta_2-\delta_0)$ obtained from fits using coherent mixing calculations for the α_0 angular correlation.

TABLE VII. Calculated cross section (in mb/sr) for the GMR and GQR with 100% EWSR at $E_x=18.7$ MeV, excited by 129 MeV α particles detected at 0°.

		*E*0		
	Satch[a] Version 1	Satch[a] Version 2	Kishimoto[b]	*E*2
Optical potential	σ (mb/sr)	σ (mb/sr)	σ (mb/sr)	σ (mb/sr)
Present	140.3	100.2	244.5	65.5
Ref. 30	99.0	134.5	120.8	72.4

[a]See Ref. 24.
[b]See Ref. 5.

branching ratio of 22±3 % reported for the ^{28}Si GQR in Ref. 15, the cross section attributable to *E*2 decay is 4.3±1.1 mb/sr. From the Legendre polynomial fits, a total p_0 decay cross section of 14.2±2.5 mb/sr was obtained, of which 9.9±2.7 mb/sr would then be *E*0 if only *E*0 and *E*2 contribute. These cross sections correspond to 7.0±1.7 % EWSR for *E*2 and 12.2±3.3 % EWSR for *E*0. In the same way, if the $p_{1,2}$ branching ratio 20±3 % for *E*2 (Ref. 15) is assumed and the cross section 11.6±2.4 mb/sr for the $p_{1,2}$ decay from the Legendre polynomial fits is used, the decay cross sections 3.9±1.0 mb/sr for *E*2 and 7.7±2.7 mb/sr for *E*0 are obtained, which correspond to 6.4±1.5 % EWSR for *E*2 and 9.5±3.3 % EWSR for *E*0.

The *E*0 and *E*2 strength and the branching ratio obtained in this study are summarized in Table V for *E*2 and in Table VI for *E*0, along with the results from the ^{24}Mg(α,γ) reaction[31] and the ^{28}Si(α,α') GQR coincidence experiment.[15] The present result for the *E*2 decay strength to the α_0 decay channel is in good agreement with both experiments. The *E*2 decay strength to the other decay channels is also in reasonable agreement with Ref. 15 within error, but the α_1 decay branch obtained is somewhat smaller than reported in Ref. 15. As shown in Table III, the decay strength of the $l=j=4$ component was strong in α_1 decay of the GQR. The dominance of $l=j=4$ component was also found in the alpha decay of the GQR in ^{28}Si (Ref. 15) and ^{16}O (Ref. 26) to the first excited state (2^+) of the residual nucleus and was explained by a strong overlap of the lp-1h configuration of the GQR with an alpha cluster ^{24}Mg$+\alpha$ $(l=2)$.[28]

The branching ratios into each of the observed channels for the *E*0 were obtained by comparing the absolute cross section of the observed *E*0 decay to the total *E*0 strength observed in the singles[5] for the same energy region. They are summarized in Table VI. The total *E*0 decay observed to the α_0, α_1, p_0, and $p_{1,2}$ decay channels corresponds to 42% of the *E*0 EWSR; 76% of the monopole strength seen in singles.[5] The α_0 and p_0 branching ratio for the *E*0 is larger than the corresponding ratio for the *E*2. This contrasts with the ^{28}Si$(e,e'c)$ results of Kihm *et al.*,[7] where the *E*0 component of α_0 decay was found to be only 40% of the *E*2 component. Their analysis is quite model dependent, however. Schmid[29] reported a microscopic calculation of the structure of the GMR in ^{28}Si, with angular momentum projected Hartree-Fock and the particle-hole model. Only 30% of the EWSR strength, which was spread over a wide excitation energy region $E_x\sim10$–56 MeV, was predicted in their model. The missing strength was attributed to the truncated configuration space employed in the calculation. From the large decay branches for the p_0 and $p_{1,2}$ channels (spin-parity for the residual states, $\frac{5}{2}^+$, $\frac{1}{2}^+$, and $\frac{3}{2}^+$) observed in the present experiment, large contributions to the transition strength may be expected from $2\hbar\omega$ 1p-1h excitations into the 3*s* and 2*d* orbits, which were not included in Schmid's[29] calculation. There have been few experimental studies of the GMR decay, but the 30% branch of the α_0 decay for the GMR in ^{40}Ca, recently found by Brandenburg *et al.*,[13] is comparable to the 18% branch obtained in the present work for ^{28}Si. The large alpha decay branch suggests that alpha clustering could be important in the GMR in light nuclei.

The singles data obtained in this experiment are consistent with those of Ref. 5, with the same integrated giant resonance cross section and the same *E*0 strength; the DWBA calculations were done with the same transition potentials and optical parameters. Thus the branching ratios obtained in the present studies which rely on the singles data of Ref. 5 should be model independent, but the absolute strengths are model dependent. As an illustration of the model dependence of the strengths, the cross sections calculated with DWBA for both a GMR and a GQR located at 18.7 MeV in ^{28}Si and excited with 129 MeV alpha inelastic scattering and detected at 0°, for differing models of the form factors and differing optical potentials are listed in Table VII. The first potential was used in the present study; the other was used in the GQR study of 120 MeV alpha inelastic scattering.[30] Although the cross sections obtained for the *E*2 are not very sensitive to the parameters, there exist large differences in the predicted *E*0 cross sections. This problem is beyond the extent of the present study, and more experimental and theoretical efforts are needed to resolve these uncertainties.

CONCLUSIONS

Proton and alpha decay from the giant resonance region ($E_x = 15.5-22.5$ MeV) of ^{28}Si was measured in coincidence with inelastic alpha particles at 0°. $E0$ and $E2$ states were selectively excited by inelastic scattering and decayed mainly to the low-lying states of the residual nuclei by emission of alpha particles and protons. The quasifree knockout process did not contribute significantly to the α_0 and α_1 decay channels in the angular range $\theta_d = 25°-155°$ of the decay detector, but did contribute in the p_0 and $p_{1,2}$ decay channels at forward angles, $\theta_d = 25°-50°$. The coincidence spectrum showed fine structure and the angular correlation showed the interference of decay amplitudes from these overlapping resonances.

The $E0$ and $E1$ strengths and the branching ratios obtained for the main decay channels are summarized in Tables V and VI. The results for $E2$ decay are in good agreement with α capture[32] and a ^{28}Si(α,α') coincidence GQR experiment.[15] The $E0$ strength (% EWSR) obtained is 9.2 ± 1.6 % for α_0, 12.2 ± 3.3 % for p_0, and $9.5+3.3$ % for $p_{1,2}$ in the 15.5–22.5 MeV excitation region and 10.7 ± 1.2 % for α_1 in the 16.7–22.5 MeV region. The total (42% of $E0$ EWSR) represents 76% of the $E0$ strength found in the singles measurement.[5] These decay strengths correspond to branching ratios, 18 ± 6 % for α_0, 24 ± 8 % for α_1, 23 ± 9 % for p_0, and 18 ± 8 % for $p_{1,2}$. The branching ratios for α_0, α_1, and p_0 exceed the expected ratio from the statistical decay calculation. In the p_0 and α_1 decay, the difference is a factor 2–4, strongly suggesting direct decay. In addition, the necessity of using a coherent treatment of the several contributions to fit the α angular correlation data also suggests the GMR in ^{28}Si decays predominantly by a direct process.[15] Similar direct contributions to decay have been observed in the GQR in ^{28}Si (Ref. 15) and in ^{58}Ni (Ref. 33).

This work was supported in part by the National Science Foundation, by the Department of Energy under Grant No. DE-FG05-86ER40256, and by The Robert A. Welch Foundation.

---

*Present address: Physikalisches Institut, Universitat Tubingen, D-7400 Tubingen, Federal Republic of Germany.

†Present address: Springer Verlag, D-1000 Berlin, Federal Republic of Germany.

[1]D. H. Youngblood, C. M. Rozsa, J. M. Moss, D. R. Brown, and J. D. Bronson, Phys. Rev. Lett. **39**, 1188 (1977).

[2]D. H. Youngblood, in *Giant Multipole Resonance,* edited by F. Betrand (Harwood, New York, 1980), p. 113.

[3]D. H. Youngblood, P. Bogucki, J. D. Bronson, U. Garg, Y.-W. Lui, and C. M. Rozsa, Phys. Rev. **23**, 1997 (1981).

[4]M. Buenerd, J. Phys. C **4**, 115 (1984).

[5]Y.-W. Lui, J. D. Bronson, D. H. Youngblood, Y. Toba, and U. Garg, Phys. Rev. C **31**, 1643 (1985).

[6]S. Kailas, P. P. Singh, A. D. Bacher, C. C. Foster, D. L. Friesel, P. Schwandt, and J. Wiggins, Phys. Rev. C **25**, 1263 (1982).

[7]Th. Kihm, K. T. Knöpfle, H. Riedesel, M. Spahn, P. Voruganti, H. J. Emirch, G. Fricke, R. Neuhausen, R. K. M. Schneider, and J. R. Calarco, in *Weak and Electromagnetic Interactions in Nuclei,* Proceedings of the International Symposium, Heidelberg, Federal Republic of Germany 1986, edited by H. V. Klapdor (Springer, New York, 1986), p. 141.

[8]H. J. Lu, S. Brandenburg, R. De Leo, M. N. Harakeh, T. D. Poelhekken, and A. van der Woude, Phys. Rev. C **33**, 1116 (1986).

[9]D. Lebrun, M. Buenerd, P. Martin, P. de Saintignon, and G. Perrin, Phys. Lett. **97B**, 358 (1980).

[10]G. Duhmal, M. Buenerd, P. de Saintignon, J. Chauvin, D. Lebrun, Ph. Martin, and G. Perrin, Phys. Rev. C **38**, 2509 (1988).

[11]Y.-W. Lui, J. D. Bronson, C. M. Rozsa, D. H. Youngblood, P. Bogucki, and U. Garg, Phys. Rev. C **24**, 884 (1981).

[12]T. Yamagata, K. Iwamoto, S. Kishimoto, B. Saeki, K. Yuasa, M. Tanaka, T. Fukuda, K. Okada, I. Miura, M. Inoue, and H. Ogata, Phys. Rev. Lett. **40**, 1628 (1978).

[13]S. Brandenberg, R. De Leo, A. G. Drentje, M. N. Harakeh, H. Sakai, and A. van der Woude, Phys. Lett. **130B**, 9 (1983).

[14]G. J. Wagner, in *Giant Multipole Resonances,* edited by F. Bertrand (Harwood, New York, 1980), p. 251.

[15]K. T. Knöpfle, H. Riedesel, K. Schindler, G. J. Wagner, C. Mayer-Böricke, W. Oelert, M. Rogge, and P. Turek, Phys. Rev. Lett. **46**, 1372 (1981); H. Riedesel, K. T. Knöpfle, K. Schindler, G. J. Wagner, W. Oclert, M. Rogge, and P. Turek, Nucl. Phys. **A454**, 85 (1986).

[16]C. M. Rozsa, D. H. Youngblood, J. D. Bronson, Y.-W. Lui, and U. Garg, Phys. Rev. C **21**, 1252 (1980).

[17]D. R. Brown, J. M. Moss, C. M. Rozsa, D. H. Youngblood, and J. D. Bronson, Nucl. Phys. **A313**, 157 (1979).

[18]J. D. Sherman, D. L. Hendrie, and M. S. Zisman, Phys. Rev. C **13**, 20 (1976).

[19]F. Zwarts, K. van der Borg, A. G. Drentje, M. N. Harakeh, W. A. Sterrenburg, and A. van der Woude, Phys. Rev. C **25**, 2139 (1982).

[20]K. T. Knöpfle and G. J. Wagner, Phys. Rev. C **27**, 2422 (1983).

[21]P. R. Bevington, *Data Reduction and Error Analysis for the Physical Sciences* (McGraw-Hill, New York, 1969).

[22]F. Pühlhofer, Nucl. Phys. **A280**, 267 (1977).

[23]A. Bohr and B. R. Mottelson, *Nuclear Structure* (Benjamin, New York, 1969), Vol. 1.

[24]G. R. Satchler, Nucl. Phys. **55**, 1 (1964).

[25]P. D. Kunz (unpublished).

[26]K. T. Knöpfle, G. J. Wagner, P. Paul, H. Breuer, C. Mayer-Boricke, M. Rogge, and P. Turek, Phys. Lett. **74B**, 191 (1978).

[27]F. Zwarts, A. G. Drentje, M. N. Harakeh, and A. van der Woude, Phys. Lett. **125B**, 123 (1983).

[28]A. Faessler, D. J. Millener, P. Paul, and D. Strottman, Nucl. Phys. **A330**, 333 (1979).

[29]K. W. Schmid, Phys. Rev. C **24**, 1283 (1981); B. Fladt, K. W. Schmid, and F. Grümmer, Ann. Phys. (N.Y.) **184**, 254 (1988).

[30]K. van der Borg, M. N. Harakeh, and A. van der Woude, Nucl. Phys. **A365**, 243 (1981).

[31]K. T. Knöpfle, G. J. Wagner, A. Kiss, M. Rogge, C. Mayer-Boricke, and Th. Bauer, Phys. Lett. **64B**, 263 (1976); K. T. Hecht and D. Braunschweig, Nucl. Phys. **A295**, 34 (1978).
[32]E. Kuhlman, K. A. Snover, G. Feldman, and M. Hindi, Phys. Rev. C **27**, 948 (1983).
[33]P. Grabmayr, G. J. Wagner, K. T. Knöpfle, H. Riedesel, P. Bogucki, J. D. Bronson, Y.-W. Lui, U. Garg, and D. H. Youngblood, Phys. Rev. C **34**, 322 (1986).